




Open Archive TOULOUSE Archive Ouverte (OATAO)

OATAO is an open access repository that collects the work of Toulouse researchers and makes it freely available over the web where possible.

This is an author-deposited version published in : <http://oatao.univ-toulouse.fr/>
Eprints ID : 19582

To link to this article : DOI: 10.1016/j.ces.2017.11.035
URL : <http://dx.doi.org/10.1016/j.ces.2017.11.035>

To cite this version : You, Xinqiang and Gu, Jinglian and Gerbaud, Vincent  and Peng, Changiun and Liu, Honglai *Optimization of pre-concentration, entrainer recycle and pressure selection for the extractive distillation of acetonitrile-water with ethylene glycol.* (2018) Chemical Engineering Science, vol. 177. pp. 354-368. ISSN 0009-2509

Any correspondence concerning this service should be sent to the repository administrator: staff-oatao@listes-diff.inp-toulouse.fr

Optimization of pre-concentration, entrainer recycle and pressure selection for the extractive distillation of acetonitrile-water with ethylene glycol

Xinqiang You^a, Jinglian Gu^b, Vincent Gerbaud^{c,*}, Changjun Peng^a, Honglai Liu^{a,*}

^a State Key Laboratory of Chemical Engineering and Department of Chemistry, School of Chemistry & Molecular Engineering, East China University of Science and Technology, Shanghai 200237, China

^b School of Chemistry and Chemical Engineering, Chongqing University, Chongqing 400044, China

^c Laboratoire de Génie Chimique, Université de Toulouse, CNRS, INP, UPS, Toulouse, France

HIGHLIGHTS

- We optimize an extractive distillation process with preconcentrator column.
- The case study belongs to the usual 1.0-1a class; min T + E heavy.
- Lowering the pressure enhances relative volatility in all columns.
- Lowering the pressure improves energy consumption and reduces costs.
- Too much entrainer recycle impurity limits distillate purity and recovery.

ABSTRACT

We optimize the extractive distillation process for separating the acetonitrile – water azeotropic mixture with ethylene glycol by using a multi-objective genetic algorithm for minimizing under purity constraints the total cost, the energy consumption and the separation efficiency. For the first time we have shown the interest of five aspects by considering them simultaneously (1) the pre-concentration column has been included and (2) there is no need to set a distillate composition constraint (like being at the azeotropic composition) in the pre-concentration column. (3) The operating pressure should be lower than 1 atm because it enhances the relative volatility for 1.0-1a class system. (4) A closed loop optimization must be run, to handle the effect of impurity in the entrainer recycle since too much impurity limits the main product recovery and purity from the extractive column. (5) All three columns process must be optimized together rather than sequentially and with multiple objectives. The studied system belongs to class 1.0-1a and the impurity of the recycled entrainer has strong effect on the purity of acetonitrile product. Overall, 17 variables are optimized; column trays, all feed locations, refluxes, entrainer flow rate and all distillate products; under purity constraints for the acetonitrile and water product and for the entrainer recycle impurity. Among nearly 400 designs satisfying the purity specifications, the design case 3 shows an energy consumption and TAC reduced by more than 20% than a literature reference case, thanks to smaller entrainer flow rate, a reduction of 32 trays and lower operating pressures. The best design is a trade-off between first a feasibility governed by thermodynamics through composition profiles and relative volatility maps and second process cost and energy demands.

Keywords:

Extractive distillation
Reduced pressure
Energy savings
Relative volatility
Multi-objective optimization
Pareto front

1. Introduction

Acetonitrile is a widely used organic solvent in the chemical industries for the purification of butadiene and fatty acid, and an

important chemical material and synthetic intermediate in the pharmaceutical industries due to its highly chemical activity. It is also employed as the mobile phase of liquid chromatography thanks to its low viscosity and chemical reactivity (Armarego and Chai, 2013). In the processes above, large amounts of acetonitrile-water mixtures are produced. They couldn't be straightly discharged or treated in biological plants because of the high price and high toxicity of acetonitrile. Therefore, the recovery of acetonitrile

* Corresponding authors.

E-mail addresses: vincent.gerbaud@ensiacet.fr (V. Gerbaud), hlliu@ecust.edu.cn (H. Liu).

Nomenclature

A_C	condenser heat transfer area [m ²]	N_R	number of theoretical stages of regeneration column
A_R	reboiler heat transfer area [m ²]	NSGA	Non-dominated Sorting Genetic Algorithm
CEPCI	chemical engineering plant cost index	GEC	modified objective function (the energy consumption per product flow rate)
$Cost_{cap}$	capital cost [10 ⁶ \$]	P	pressure [Hgmm] [atm]
$Cost_{ope}$	operating cost [10 ⁶ \$]	P_0	pressure of the pre-concentration column
$Cost_{CA}$	column annual cost [10 ⁶ \$]	P_1	pressure of the extractive column
$Cost_{HA}$	cost of heater for cooling recycling entrainer [10 ⁶ \$]	P_0	pressure of the entrainer regeneration column
D	distillate flow [kmol/h]	PSD	pressure-swing distillation
D_0	distillate flow of pre-concentration column	Q_{c0}	condenser heat duty of pre-concentration column [MW]
D_1	distillate flow of extractive column	Q_{c1}	condenser heat duty of extractive column [MW]
D_2	distillate flow of regeneration column	Q_{c1}	condenser heat duty of regeneration column [MW]
Diameter	diameter of column	Q_{HA}	heat duty of heater for cooling recycling entrainer [MW]
E	entrainer	Q_{r0}	reboiler heat duty of pre-concentration column [MW]
E_{ext}	the efficiency indicator of extractive section	Q_{r1}	reboiler heat duty of extractive column [MW]
e_{ext}	the efficiency indicator of per tray in extractive section	Q_{r2}	reboiler heat duty of regeneration column [MW]
	e_{ext}	R	reflux ratio
ED	extractive distillation	R_0	reflux ratio of pre-concentration column
EG	ethylene glycol	R_1	reflux ratio of extractive column
F	feed flow rate [kmol/h]	R_2	reflux ratio of entrainer regeneration column
F_2	feed flow rate of the regeneration column [kmol/h]	T	temperature [K]
F_{AB}	original azeotropic mixtures feed flow rate [kmol/h]	TAC	total annual cost
F_E	entrainer feed flow rate [kmol/h]	W_2	bottom liquid flow rate of entrainer regeneration column [mol/h]
F_E/F	feed ratio, continuous process	x_D	distillate fraction
Height	height of column	x_i	liquid mole fraction of component i
I_{cs}	column shell investment cost [10 ⁶ \$]	x_F	original mixture liquid mole fraction
I_{HE}	heat exchanger investment cost [10 ⁶ \$]	x_E	entrainer liquid mole fraction
k	product price factor for A vs B	$x_{p,lower}$	product mole fraction at the lower feed tray of the extractive section
LP	low pressure	$x_{p,upper}$	product mole fraction at the upper feed tray of the extractive section
MP	middle pressure		
HP	high pressure		
m	energy price difference factor for condenser vs reboiler		
N	number of theoretical stages		
N_E	number of theoretical stages of extractive column		
N_{FE}	entrainer feed stages		
N_{FF}	original mixture feed stages		
N_{FP}	feed stages of pre-concentration column		
N_{FR}	feed stages of entrainer regeneration column		
N_p	number of theoretical stages of pre-concentration column		

Greek letters

α_{ij} volatility of component i relative to component j

trile from its aqueous solution is an emerging problem from the views of environment and economics. However, it is impossible to separate acetonitrile from its aqueous solution by conventional distillation since there is an azeotrope between acetonitrile and water with 67.3% mol acetonitrile in the azeotrope at 349.9 K under atmospheric pressure. Consequently, advanced distillation technologies like pressure swing distillation or extractive distillation are needed (Doherty and Knapp, 1993).

Pressure swing distillation (PSD) can be employed to separate pressure-sensitive minimum-boiling or maximum-boiling azeotropic mixtures without adding a third component called entrainer (Luyben, 2012). It exhibits the advantages of no entrainer impurity in the product stream and the energy-savings potential of carrying out a fruitful heat integration. Fortunately, the azeotrope of acetonitrile and water is pressure sensitive and it could be separated by PSD. Repke et al. (2005) studied the PSD process for separating acetonitrile-water and analyzed the process operation performance, but no process energy consumption and total annual cost (TAC) was mentioned. Huang et al. (2008) investigated the rectifying/stripping sections type heat integration in PSD columns for separating acetonitrile-water mixture, and they found that it failed to compete with the simple condenser/reboiler type heat integration process for the studied case.

Extractive distillation (ED) is another alternative in which the entrainer is fed at a different location than the main mixture, bringing an additional extractive section in the column, between the usual stripping and/or the rectifying sections (Rodriguez-Donis et al., 2009). In the extractive section, the entrainer should interact differently with the azeotropic components, giving rise to an increase in the relative volatility of the original components. The ED process is widely used among process to separate azeotropic mixtures because of low energy consumption and the flexible selection of possible entrainers (Mahdi et al., 2015).

Acosta-Esquivarosa et al. (2006) studied the recovery of acetonitrile from its aqueous solution by combining solvent extraction and batch distillation process with butyl acetate as solvent. Liang et al. (2014) optimized the conventional ED process for acetonitrile-water separation with ethylene glycol (EG) as entrainer by sequential iterative optimization procedure, and the process energy cost was reduced by 16% through combining the pre-concentration column with a preset distillate output and entrainer recovery column.

For the design of an ED process, there are two main issues: entrainer selection and process optimization. The entrainer selection is an important step since the effectiveness of separation was strongly relied upon the interactions between entrainer and azeotropic mixture. Gerbaud and Rodriguez-Donis (2014) have

reviewed the entrainer selection rules along with the process feasibility assessment for the separation of minimum or maximum boiling azeotropes with light, intermediate or heavy entrainers, depending on the classification of the studied system. Then, once a classification is considered, the process optimization is usually undertaken under target purity and recovery constraints, either minimizing solely the process energy cost or the total annual cost. Less commonly a multi-objective optimization is performed by targeting energy cost, TAC and other goals like thermodynamic efficiency (Ortiz and Oliveira, 2014) or CO₂ emissions (You et al., 2016a).

Overall, the optimization issue consists in finding suitable operating parameters. This is a routine procedure in most recent published works, but not with the same level of accuracy. Very often, some parameters are fixed, a single objective is targeted or the optimization is not performed globally. Typically, the columns tray numbers, main feed and entrainer feed tray locations, reflux ratios are optimized sequentially (Arifin and Chien, 2008; De Figueiredo et al., 2011 among others). But, other parameters should now be considered systematically. Recently we showed that for the separation of minimum boiling azeotrope with a heavy entrainer by ED, a lower pressure in the extractive section improves the azeotropic components relative volatility and reduces TAC by You et al. (2015a) and Luyben (2016). Some authors have also noticed that a properly designed column usually exhibit features related to the entrainer ability to enhance volatility. Hence, they have solved multi-objective problem including the maximization of a separation efficiency indicator (You et al., 2015a, 2015b), or added additional constraints to a mono-objective problem like the entrainer content on the solvent feed tray (De Figueiredo et al., 2015a, 2015b). Furthermore, several authors have shown the importance of optimizing the extractive distillation column together with the entrainer regeneration column (Luyben and Chien, 2011) and to do so simultaneously (Kossack et al., 2008; García-Herreros et al., 2011; You et al., 2015a). You et al. (2016b) recently showed that one motivations for that is because the entrainer recycle impurity sets limitations on the achievable product purity and recovery yield because of the column material balances interactions.

Regarding the studied case we use for illustration, Liang et al. (2014) reported a sequential optimization of the acetonitrile – water extractive distillation process with ethylene glycol, incl. a preconcentration column and a recovery column. They assumed (i) that all columns operated at 1 atm, (ii) the purity of the distillate in the pre-concentration column as 65%, (iii) the recycling entrainer purity equal to 99.999%, and the columns were optimized one at a time. Based on our literature survey, those assumptions on the process would affect the optimization results of the extractive distillation process.

In this paper, we waive the above assumptions and with the aim of showing how that can improve the design of the ED process for acetonitrile-water with EG as entrainer, we perform a multi-objective optimization problem solved with the help of a genetic algorithm method. The five aspects not yet considered together in the literature and referring to the flowsheet shown in Fig. 1 are the following: (1) is the pre-concentration column necessary? (2) the composition in the distillate of the pre-concentration column is a variable rather than specified as done in literature (Liang et al., 2014). (3) the operating pressures of all three columns become optimization variables. (4) by optimizing the process flowsheet in closed loop, the impact of the purity of recycling entrainer in W_2 on the process feasibility in terms of product purity and recovery is taken into account. (5) all three pre-concentration, extractive and regeneration columns are optimized simultaneously with the use of a modified energy cost objective function GEC in addition to the total annual cost. Liang's design is chosen as the base case for the sake of comparison. Notice that the process needs

a makeup entrainer to compensate its losses with the products. As its flow rate value is not known beforehand, we set it as usual, equal to the entrainer losses, which could be obtained by combining the entrainer loss streams ED1 and ED2 after sharp splits by using virtual SEP1 and SEP2 on the two product distillates D_1 and D_2 as shown in Fig. 1, respectively.

The paper is organized as follow. Section 2 describes the multi-objective optimization problem, its solving and details the objective functions. Section 3 presents the results in terms of multi-criteria Pareto front and compare the final solutions with the base case. In Section 3, we analyze the final solutions with respect to the extractive separation efficiency and the relative volatility profiles. We conclude in Section 4 by discussing the importance of the five design issues aforementioned on the solutions.

2. Multi-objective genetic algorithm and process evaluation

2.1. Multi-objective genetic algorithm

As a consequence to the choices we make, seventeen variables are optimized: the tray numbers of the pre-concentration, extractive and regeneration columns N_p , N_E and N_R ; the column feed locations N_{FP} , N_{FE} , N_{FF} , N_{FR} ; the distillates, reflux ratios and operating pressures D_0 , D_1 , D_2 ; R_0 , R_1 , R_2 ; P_0 , P_1 , P_2 , and the entrainer flow rate F_E , respectively.

The studies of Rangaiah et al. review the limitations and the advantages of multi-objective optimization in the design and operation of energy efficient chemical processes (Rangaiah, 2009; Rangaiah et al., 2013, 2015). Compared with the sequential iterative optimization procedure dominantly used in the extractive distillation literature (see Section 1), genetic algorithms are attractive because they are able to perform a multi-objective optimization where the influence of each parameter on the solution is evaluated simultaneously rather than sequentially. Unlike single objective optimization method as done in the study of Kossack et al. (2008), multi-objective genetic algorithm provides a list of solutions satisfying the purity constraints but with different operating parameters. Pareto fronts displaying the results give hints at the flexibility on choosing design parameters enabling a feasible process. Although the multi-objective genetic algorithm is computer intensive, it is less sensitive to initialization and requires no explicit information of the mathematical model or its derivatives because the algorithm is based on a direct search method (Leboreiro and Acevedo, 2004).

The multi-objective genetic algorithm called “gamultiobj” in Matlab was linked with Aspen plus V7.3 process simulator. Non-dominated Sorting Genetic Algorithm (NSGA) II is the method we used as it proved successfully in the optimization of several distillation processes (You et al., 2015a; Bravo-Bravo et al., 2010). The rigorous model *Radfrac* including MESH equations in Aspen Plus was adopted for the process simulation. As the result of the GA multi-objective optimization, the Pareto front displays a set of non-dominated, optimal designs (Gomez et al., 2010) that satisfy the specification of the product purities. Notice that any design belonging to the Pareto front means that it couldn't be improved through one objective function without worsening the other objectives.

2.2. Process evaluation

2.2.1. Economical evaluation

The total annual cost (TAC) is used for economically evaluating the different designs since it is a trade-off between capital cost and operating cost. It is computed from the following formula:

$$TAC = \frac{\text{capital cost}}{\text{payback period}} + \text{operating cost} \quad (1)$$

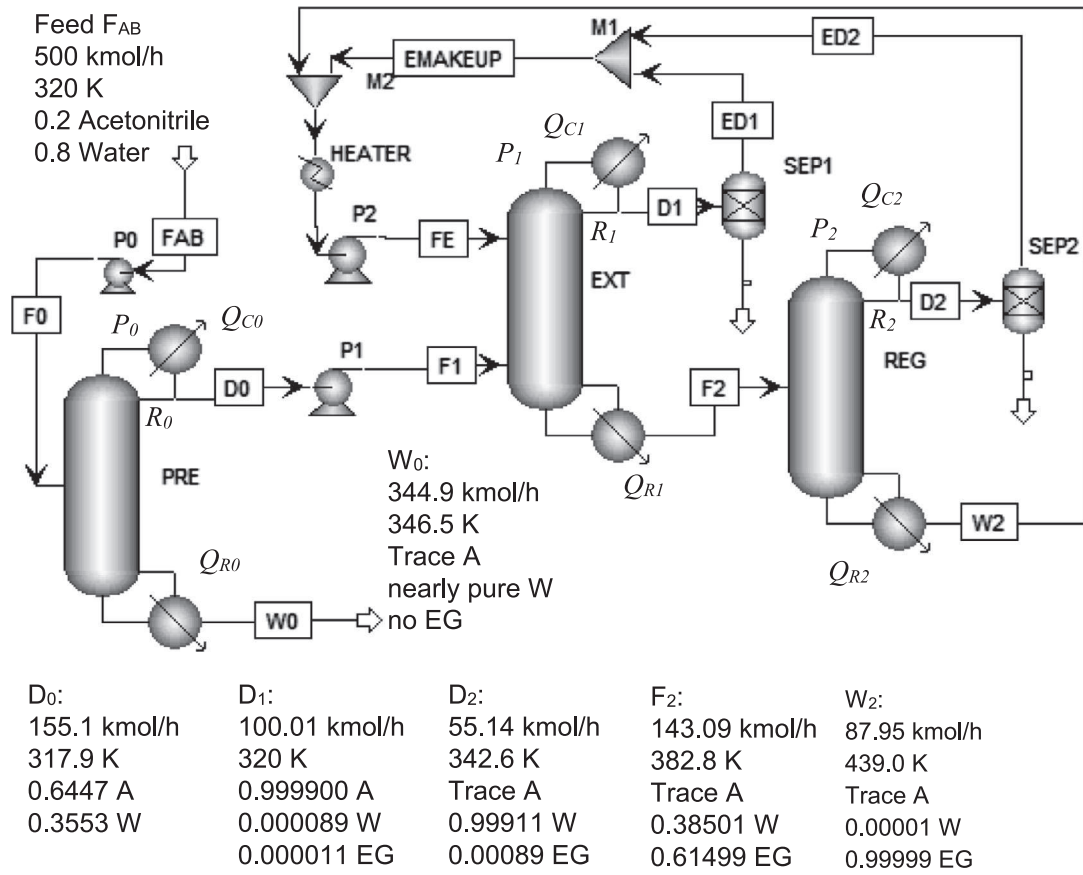


Fig. 1. Three columns closed loop flowsheet of acetonitrile (A) – water (W) extractive distillation with ethylene glycol (EG) as entrainer. The data correspond to our best design, named case 3.

The operating cost contains the energy cost in reboiler and condenser. The capital cost consists of the column shell, tray and heat exchanger and the related capital cost formulas are shown in Appendix A. The Douglas' cost formulas (Douglas, 1988) are transferred into CEPCI inflation index and employed for calculating the process capital cost. The CEPCI (2016) with value of 567.3 and a three-year payback period are selected. Notice that when the operating pressure is not higher than 3 atm, the effect of pressure on the capital cost could be neglected according to Douglas' cost formulas (Douglas, 1988). Similarly, the capital cost of vacuum pressure conditions that we investigate is considered negligible compared to the costs of the other pumps shown in Fig. 1. The heat exchanger for cooling the recycling entrainer is taken into account in order to emphasize its effect on the process. Notice that the tray number is counted from top to down of the column, and the condenser and reboiler are regarded as the first and last tray. The tray efficiency of 85% (De Figueiredo et al., 2015b) is used for calculating TAC. Other costs such as the liquid delivery pumps, pipes, valves are neglected.

2.2.2. Energy consumption evaluation

With the aim of optimizing the three columns in Fig. 1 simultaneously rather than in sequence, we define a global energy consumption function (GEC) is as follow.

$$GEC = \frac{M_0 \cdot Q_{R0} + M_1 \cdot Q_{R1} + M_2 \cdot Q_{R2} + m \cdot Q_{C0} + m \cdot Q_{C1} + m \cdot Q_{C2}}{D_1} \quad (2)$$

The meaning of the variables is shown in Fig. 1. The factor m represents the energy price difference for condenser vs reboiler and its value equals to (cooling water price)/(low pressure steam price)

= 0.036 (You et al., 2015a, 2015b). The factor M reflects the prices of different pressure heat steams and equals 1, 1.065 or 1.280 when low, middle or high pressure steam is used, respectively. The subscripts 0, 1 and 2 refer to the pre-concentration, the extractive and the regeneration column, respectively. The process utilities are shown in Table 1.

The meaning of GEC is the energy consumption used per product unit flow rate (kJ/kmol). It accounts for all the columns and also reflects the weight coefficient of the reboiler - condenser heat duty. The energy consumption function GEC could be easily expanded to more columns process.

The GEC formula contains the valuable distillate products streams in the denominator. For our case study, D_2 is no need to be treated at denominator of GEC since D_2 product is water. But constraint 2 is necessary for reducing the entrainer EG losses since according to the interrelationships among distillates (You et al., 2016b) it impacts the process ability to achieve the desired purity in D_1 . Besides, constraint 2 also sets a lower limit to the loss of acetonitrile in D_2 which should improve the recovery of acetonitrile in D_1 . Constraint 1 then helps keeping a high acetonitrile purity. Con-

Table 1
Process utilities (Zhu et al., 2015).

Name	Pressure/MPa	Temperature/K	Price/\$/GJ
LP steam	0.5	433	7.72
MP steam	1.0	457	8.22
HP steam	1.5	527	9.88
Cooling water	0.1	298	0.278

straint 3 works for avoiding too much acetonitrile loss in the bottom liquid of the pre-concentration column. In introduction, we insisted on the recycling entrainer purity in stream W_2 that should be compatible with constraint 1 on the main product. A fourth constraint could be set accordingly. Instead, we adopt a solving strategy where the optimization problem handled by the genetic algorithm monitors the process simulation carried out by Aspen plus software in closed loop. The Wegstein tear method in Aspen plus software handles the purity and flowrate of the recycling entrainer stream which is automatically determined through the simulation process to match the constraints at the optimization problem level.

2.2.3. Separation efficiency evaluation

In the extractive distillation process, monitoring the amount of entrainer in the middle (extractive) section, between the entrainer and main feed tray locations, is vital for separating azeotropic mixture. Knapp and Doherty (1994) discussed the minimal amount of entrainer and De Figueiredo et al. (2015a, 2015b) used the amount of entrainer on the entrainer feed tray as a constraint for designing the column. In this work we use the efficiency indicator of extractive section E_{ext} and the efficiency indicator of per tray in extractive section e_{ext} that we proposed recently (You et al., 2015a). They represent the ability of the extractive section to discriminate the desired product between the top and the bottom of the extractive section. The efficiency indicator per tray e_{ext} is supplementary to E_{ext} for dealing the different designs with different entrainer-to-feed flow rate ratios, different reflux ratios and different tray numbers in the extractive section:

$$E_{ext} = x_{p,upper} - x_{p,lower}^* \quad (3)$$

$$e_{ext} = \frac{E_{ext}}{N_{ext} - 1} \quad (4)$$

where $x_{p,upper}$ is the product mole fraction at the upper feed tray of the extractive section and $x_{p,lower}^*$ represents the product mole fraction at the lower feed tray of the extractive section. In this study, the value of $x_{p,lower}$ is taken from one tray higher than the lower feed location in order to avoid the effect of the original composition in the main feed on the efficiency indicators. And N_{ext} is the tray number of the extractive section. Notice that the entrainer feed tray is counted into N_{ext} and the main feed tray is excluded.

3. Results and discussions

3.1. Problem setting

A 500 kmol/h acetonitrile-water mixture (F_{AB}) was fed to the extractive column at 320 K with a mole composition of 20% acetonitrile, the same as that in the study of Liang et al. with the aim of comparison. The ternary vapor-liquid equilibrium of the system acetonitrile-water with EG is modelled similarly to Liang's literature work (Liang et al., 2014) for the sake of comparison. The NRTL thermodynamic model with the Aspen Plus built-in binary parameters (See Table A in Appendix B) was used for the liquid phase while the vapor phase was assumed to be as a perfect gas.

In the multi-objective problem, the global energy cost GEC and TAC are minimized while the two efficiency indicators E_{ext} and e_{ext} are maximized.

$$\begin{cases} \min TAC \\ \min GEC \\ \max E_{ext} \\ \max e_{ext} \end{cases} \quad (5)$$

subject to :

$$\begin{aligned} x_{\text{acetonitrile}, D_1} &\geq 0.9999 \\ x_{\text{water}, D_2} &\geq 0.999 \\ x_{\text{water}, W_0} &\geq 0.999 \end{aligned}$$

From the economical view, the desired design is the one with the minimum TAC although four objectives are used. The logic of a multiobjective optimization comes from an earlier paper (You et al., 2015b) where we showed that the design solutions corresponding to the minimum TAC or to the minimum energy cost are different. The energy consumption GEC objective could not be solely employed to determine the tray number of columns, but it is useful for finding the variables once the column tray number was fixed. And like TAC, it is also a practical standard of comparison among different designs. There are several reasons for adding efficiency indicators as objectives. They concern the extractive section, which drives the feasibility of the whole process (Knapp and Doherty, 1994; Rodriguez-Donis et al., 2009). You et al. (2015b) showed that they are useful to compare seemingly TAC or energy equivalent designs and the solutions displayed in the Pareto fronts hint at the flexibility on choosing design parameters enabling a feasible process. Besides, the separation efficiency per tray e_{ext} is used herein to avoid excessive trays employed in the extractive section when E_{ext} only is maximized.

The purpose of the constraints is explained below. The GEC formula contains the valuable distillate products streams in the denominator. For our case study, D_2 is no need to be treated at denominator of GEC since D_2 product is water. But constraint 2 is necessary for reducing the entrainer EG losses since according to the interrelationships among distillates (You et al., 2016b) it impacts the process ability to achieve the desired purity in D_1 . Besides, constraint 2 also sets a lower limit to the loss of acetonitrile in D_2 which should improve the recovery of acetonitrile in D_1 . Constraint 1 then helps keeping a high acetonitrile purity. Constraint 3 works for avoiding too much acetonitrile loss in the bottom liquid of the pre-concentration column. In introduction, we insisted on the recycling entrainer purity in stream W_2 that should be compatible with constraint 1 on the main product. A fourth constraint could be set accordingly. Instead, we adopt a solving strategy where the optimization problem handled by the genetic algorithm monitors the process simulation carried out by Aspen plus software in closed loop. The Wegstein tear method in Aspen plus software handles the purity and flowrate of the recycling entrainer stream which is automatically determined through the simulation process to match the constraints at the optimization problem level.

The population and the crossover and mutation fractions parameters of the genetic algorithm were tuned after several preliminary tests. After tuning, 400 individuals, 0.9 for crossover fraction and 0.1 for mutation fraction were employed. When the number of generations reaches 480, the four objective functions could not be further improved and the optimization stops. More about the solving progress along the generations is available in Table C in Appendix B. The stand-alone computer and its CPU was Intel (R) core i7 (3.6 GHz) with 4Gbytes memory. It took about 12 days to get results, with an average of 5 s for each of the 1.92×10^5 Aspen plus simulations. This is much longer than deterministic optimization which can be carried out in minutes or hours (Kossack et al., 2008) but in addition to a robustness to initial conditions and applicability to unknown structure problem, the genetic algorithm results offer a large panel of feasible design parameters which can be analyzed to gain further knowledge on the process.

The seventeen variables being optimized are $N_p, N_e, N_R, N_{FP}, N_{FE}, N_{FR}, D_0, D_1, D_2, R_0, R_1, R_2, F_E, P_0, P_1, P_2$, referring to Fig. 1. The value ranges encompass those of the reference design (see Table 2 below) and are [3–5] for N_p , [20–70] for N_e , [3–30] for N_R , [2–0] for N_{FP} , [2–20] for N_{FE} , [15–60] for N_{FR} , [2–20] for N_{FR} , [140.00–160.00] kmol/h for D_0 , [99.00–101.00] kmol/h for D_1 , [0.00–400.00] kmol/h for D_2 , [0.001–1.000] for R_0 , [0.010–1.500] for R_1 , [0.010–1.000] for R_2 , [20.0–250.0] kmol/h for F_E , [0.3–1.5] atm for P_0, P_1 and P_2 . The entrainer flow rate F_E exhibits the entrainer-to-feed reflux ratio as

Table 2

The reference design and its modification.

	Case 1 ^a	Case 2
Pressure drop/atm	0.0068	0.0068
N_P	16	
N_E	54	
N_R	19	
N_{FP}	8	
N_{FE}	6	
N_{FF}	46	
N_{FR}	10	
D_0 /kmol/h	153.793	
D_1 /kmol/h	99.97	
D_2 /kmol/h	53.823	
R_0	0.0884	0.155
R_1	0.466	0.747
R_2	0.225	0.276
F_E /kmol/h	145	
P_0 /atm	1	
P_1 /atm	1	
P_2 /atm	1	
$x_{\text{acetonitrile},D1}$	0.98749	0.99996
$x_{\text{water},D2}$	0.99526	0.99995
$x_{\text{water},W0}$	0.99631	0.99991
GEC /kJ/kmol	199285.0	213205.6
$TAC/10^6 \$$	1.669	1.781
E_{ext}	0.219	0.178
e_{ext}	0.0053	0.0043

^a Design using Liang's parameters (Liang et al., 2014) and adding a pressure drop.

the flow rate of azeotropic mixture is constant. We set 0.3 atm as the lower limit of the operating pressure as below that value, we cannot use cheap cooling water at the condenser. The low bound of F_E is set based on the minimal amount of entrainer to break the azeotrope of acetonitrile–water at 0.3 atm. It is greater than 20 kmol/h, based on the procedure in Gerbaud and Rodriguez-Donis (2014), that comes from the knowledge of the intersection of the univolatility curve $\alpha_{\text{Acet.,Water}} = 1$ with the EG–acetonitrile edge and assuming a positive reflux ratio and distillate flow rate near 100 kmol/h.

3.2. Design results and discussions

3.2.1. Designs with pressure drop per tray

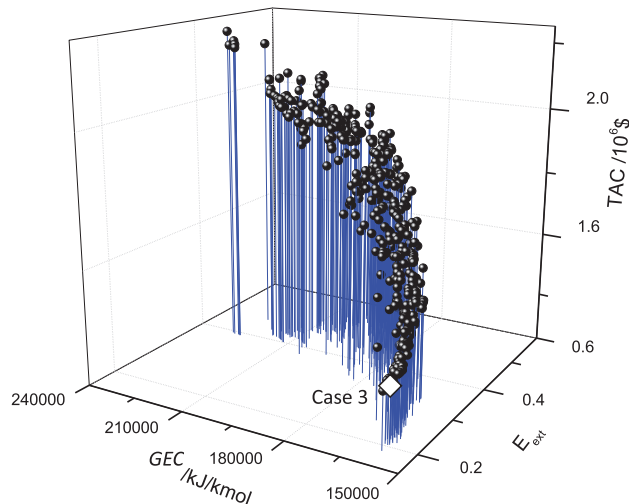
Since the azeotrope of acetonitrile–water is pressure-sensitive, it is necessary to consider the pressure drop per tray. The pressure drop per tray for the three columns employed herein is 0.0068 atm

(Luyben and Chien, 2011). This impacts all columns and induces feed composition changes. Indeed, the literature design with no pressure drop (Liang et al., 2014) was found unable to achieve the product purities when simply considering pressure drop: case 1 in Table 2 show that the acetonitrile purity is below the specified value. Therefore, we optimized the three reflux ratios for meeting the product purities specifications by using two-step optimization procedure (You et al., 2015a) while keeping other variables the same as case 1. The modified design called case 2 is also shown in Table 2. The sizing parameters and the cost data of the designs case 1 and 2 are shown in Table B in Appendix B. Case 2 is 7% less profitable and 7% more energy demanding. These numbers are significant and highlight the need to consider pressure drop systematically.

3.2.2. Pareto front of the three columns process design solutions

The progress of the NSGA II convergence is shown in Table C in Appendix B. In the final Pareto front, we obtained 400 designs that meet the purity specifications and constraints. There are 169 designs with a TAC lower than that of case 1 and 228 designs with a TAC below that of case 2. The operating pressures of the three columns were all 0.3 atm in the whole 400 designs although its value range was set from 0.3 atm to 1.5 atm. The main reasons are that the relative volatility of acetonitrile over water and the azeotropic composition of acetonitrile increases under lower pressure. That behaviour highlights the need to consider the operating pressures of the three columns as variables. It was also noticed that lowering the pressure enhanced the relative volatility of the acetonitrile over water at the same entrainer flow rate, and by promising an easier separation, it could lead to the reduction of TAC for the studied system, which belongs to 1.0-1a extractive separation class. Lowering the pressure has been employed for other 1.0-1a class, such as the acetone – methanol separation with water, the Diisopropyl Ether – Isopropyl Alcohol separation with 2-methoxyethanol and 2-methoxyethanol – toluene separation with DMSO (You et al., 2015a, 2016b; Li et al., 2017).

Results belonging to the Pareto front of the stochastic optimization are displayed in Figs. 2–4. Fig. 2 shows the Pareto front of the acetonitrile–water–EG system, TAC versus GEC and E_{ext} . Fig. 3 shows the effects of key variables R_1 and F_E in the extractive column on the process TAC. The lowest TAC design, namely case 3, is shown as a white diamond in Figs. 2 and 3. More design parameters of case 3 are presented later in Table 4. Case 2 satisfies the three purity constraints but does not belong to the Pareto front because it pro-

**Fig. 2.** Pareto front of the acetonitrile–water–EG system, TAC versus GEC and E_{ext} , the red diamond indicates case 3.

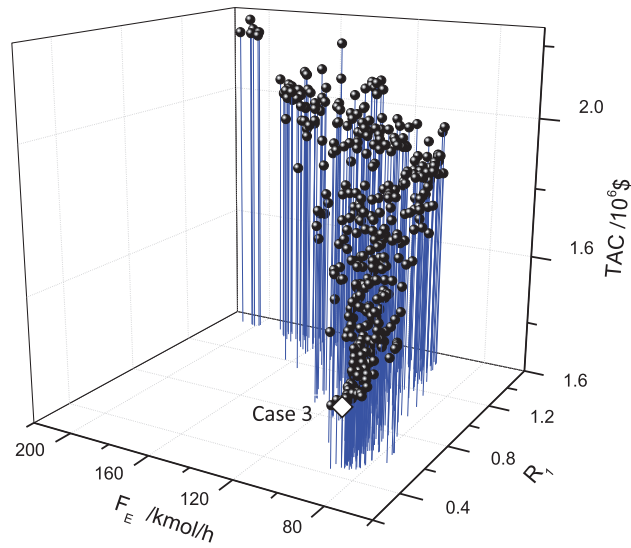


Fig. 3. Effects of key variables R_1 and F_E in the extractive column on the process TAC of the acetonitrile–water–EG system, TAC versus R_1 and F_E .

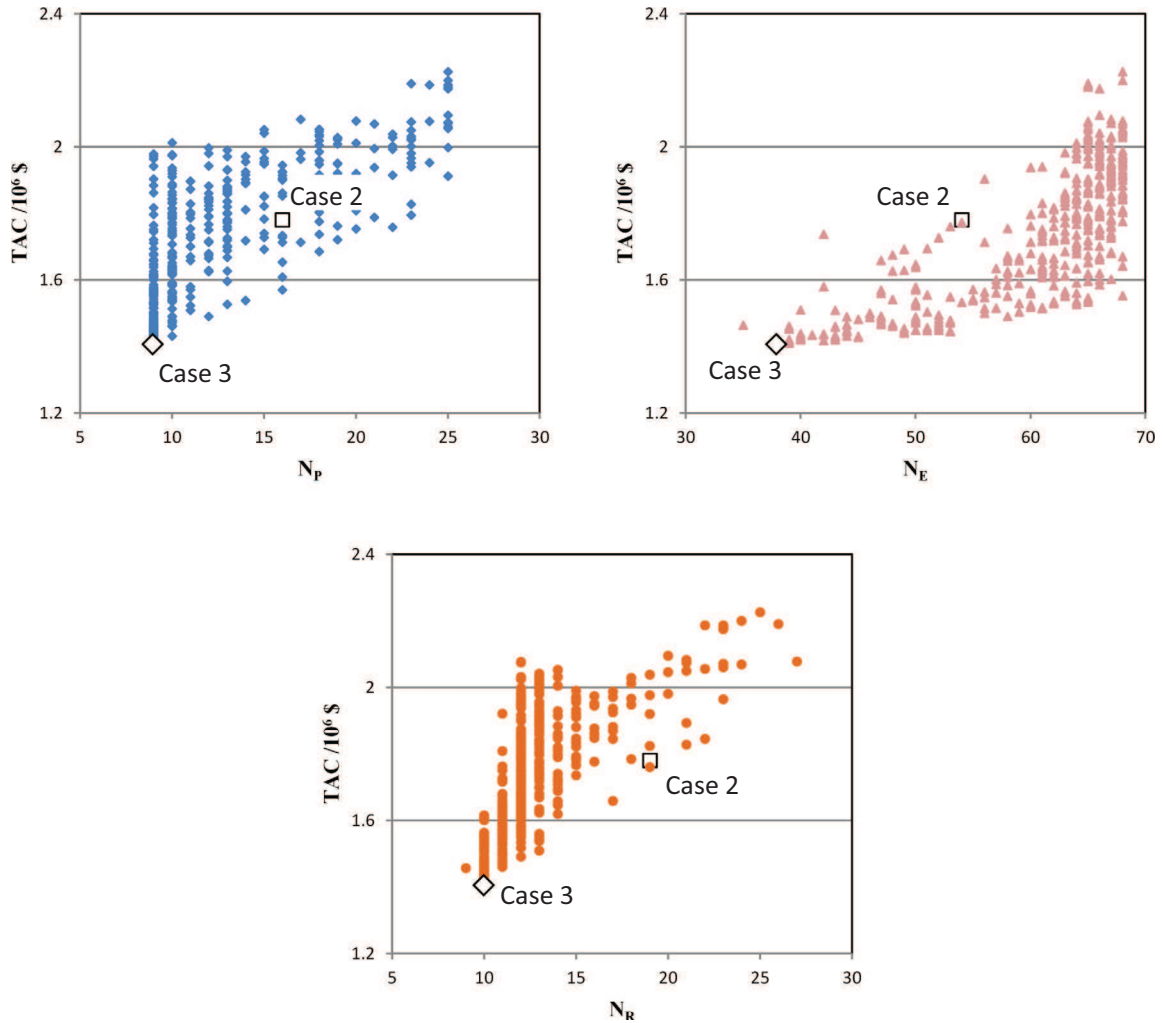


Fig. 4. Effects of tray numbers of the three columns on the process, the white box indicates the reference design case 2.

duces less distillate (see Section 3.2.4). Compared with case 2, case 3 design essentially improves greatly the TAC and GEC while necessitating much less entrainer, less heat exchange and less tray num-

bers in all three columns, and producing more distillate. Although the recycling entrainer purity was not set as a constraint for reasons given in Section 2.2.2, all designs showed a very high purity,

Table 3

Azeotropic temperature and acetonitrile azeotropic composition for case 1, 2 and 3.

	Pressure/ atm	$x_{\text{acetonitrile}, D_0}$ / mole	$T_{\text{azeo}}/$ (°C)	$x_{\text{azeo}}/$ mole	α_{AB}^a
Case 1 and 2	1	0.650	349.96	0.673	1.07
Case 3	0.3	0.6447	317.79	0.765	1.46

^a The relative volatility of acetonitrile (A) over water (B) at distillate stream (D_0) of pre-concentration column.

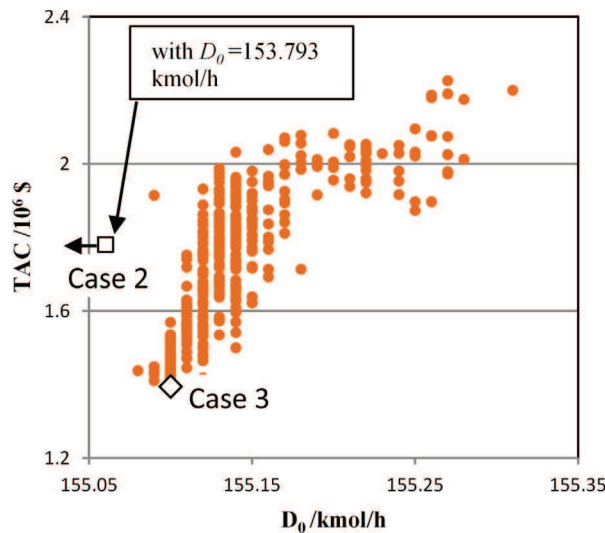
which we explained was necessary as recycling impurities might prevent the design to achieve high recovery and purity of the products in distillates D_1 and D_2 .

From Fig. 2, we know the followings: (1) The design case 3 is the one with the lowest TAC (1.410×10^6 \$) and a GEC (158440.1 kJ/kmol). The lowest energy consumption design (case 4 in Table 3) with GEC (156628.6 kJ/kmol) exhibits a higher TAC (1.445×10^6 \$) than case 3. This demonstrates that GEC and TAC are consistent but not equivalent to be interchangeable, thus motivating our solving of a multi-objective problem. Compared to the modified literature design (case 2), case 3 displays a 20% reduction of the TAC. (2) The efficiency indicator E_{ext} decreases following the decrease of GEC and TAC. This happens because E_{ext} is related to the composition profile in the extractive section and that is strongly influenced by the entrainer flow rate and the reflux ratio of extractive column. In return, F_E and R are the dominant parameters through the column size and the reboiler heat in the global energy cost and TAC evaluation. In agreement with the literature (You et al., 2015b), maximizing the separation efficiency cannot be the only parameter driving the design.

From Fig. 3, we observe that (1) TAC increases with the increase of F_E and R_1 . The main reason is that a high F_E infers a high energy cost in the regeneration column and TAC increases consequently. (2) The economically feasible value range (case 3 minimum TAC + 10%) of the entrainer flow rate is (80–90 kmol/h), namely, (0.16–0.18) for F_E/F . This value is nearly 38% lower than that (0.29) in literature's case 2. Below $F_E = 76$ kmol/h, no solution is found, which much greater than the minimal entrainer amount necessary to break the azeotrope of acetonitrile-water.

3.2.3. Effects of tray numbers

Fig. 4 shows the influence of the tray numbers of each of the three columns on the process total annual cost. The white box represents the reference design case 2.

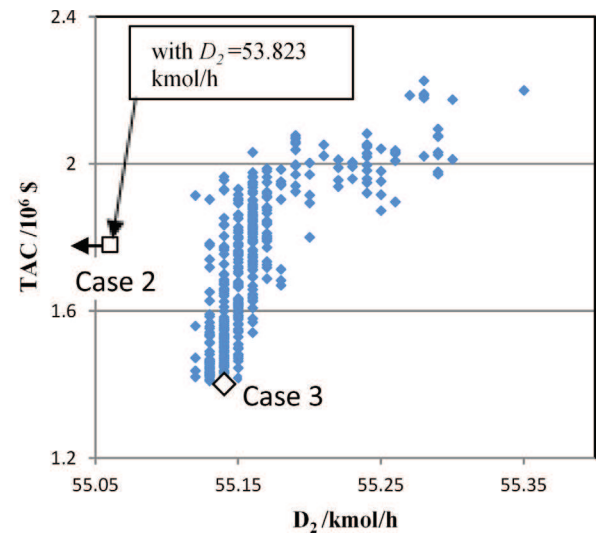
**Table 4**

Design parameters of the three columns extractive distillation process for the separation of acetonitrile – water with EG.

	Case 3	Case 4	Case 5	Case 6
N_P	9	9	18	25
N_E	38	53	67	68
N_R	10	10	18	25
N_{FP}	2	2	2	2
N_{FE}	4	4	4	4
N_{FF}	29	37	50	17
N_{FR}	4	4	4	5
D_0 /kmol/h	155.10	155.11	155.16	155.27
D_1 /kmol/h	100.01	100.01	100.01	100.01
D_2 /kmol/h	55.14	55.15	55.16	55.28
R_0	0.001	0.001	0.001	0.046
R_1	0.488	0.463	1.497	1.489
R_2	0.149	0.135	0.324	0.391
F_E /kmol/h	88.0	85.2	101.0	203.0
P_0 /atm	0.3	0.3	0.3	0.3
P_1 /atm	0.3	0.3	0.3	0.3
P_2 /atm	0.3	0.3	0.3	0.3
$x_{\text{acetonitrile}, D_0}$	0.6447	0.6447	0.6445	0.6440
$x_{\text{acetonitrile}, D_1}$	0.9999	0.9999	0.9999	0.9999
x_{water, D_2}	0.9991	0.9991	0.9998	0.9996
GEC/kJ/kmol	158440.1	156628.6	200728.3	228128.3
TAC/ 10^6 \$	1.410	1.445	1.948	2.226
E_{ext}	0.211	0.213	0.553	0.394
e_{ext}	0.0081	0.0063	0.0118	0.0281

The Pareto front in Fig. 4 show that for the pre-concentration column no design was found with N_P lower than 9 well over the lower bound set at 2 for N_P , or greater than 25 (the upper bound). Designs with $TAC < TAC_{\min} + 10\%$ require N_P between 9 and 13. Recall that the reference case 2 has $N_P = 16$. In addition, even at $N_P = 16$, there are still five better designs with a lower TAC than that of case 2. That shows the need to optimize the pre-concentration column.

For the extractive column, the potential of improvement compared to the literature reference is huge. One design in the Pareto front goes as low as $N_E = 35$. Design matching the product purity constraints and high recovery are found with N_E as many as 69. But the lowest TAC design (case 3) $N_E = 38$ is close and the range spanning designs with $TAC < TAC_{\min} + 10\%$ goes up to 53. Case 2 value (54) is close. The results confirm that employing too many trays in the column will lead to the increase of capital cost and TAC, but that N_E is not a very sensitive variable for the TAC. The main reason is that when performing a full optimization of the whole column sequence, the reflux ratio R_1 and the entrainer flow

**Fig. 5.** Effects of distillates on the process, the white box indicates the case 2.

F_E can be varied while changing N_E in order to achieve a low TAC and match the specifications. Varying R_I on the TAC is mainly reflected by the reboiler duty of the extractive column, whereas the effect of altering F_E on the TAC is mostly represented by the reboiler duty of the regeneration column. Hence, the effects on TAC of changing the number of trays in the extractive section N_E affects the regeneration column cost. This confirms the importance to optimize all the columns together.

Regarding the regeneration column, the trend is similar to the pre-concentration column. The range encompassing designs having $TAC < TAC_{min} + 10\%$ spans only 5 trays, from 9 to 13. The minimum TAC is found for $N_R = 10$, whereas case 2 value ($N_R = 19$) is far, showing how the TAC was improved by our multi-objective optimization.

3.2.4. Effects of the distillate flow rates on the process

The effects of the distillates of the pre-concentration and regeneration columns (D_0 and D_2) on the process TAC are shown in Fig. 5. For the distillate of extractive column D_1 , all the Pareto front solutions found a constant value 100.01 kmol/h even though it was allowed to vary from 99.00 to 101.00 kmol/h as mentioned in Section 3.2.2.

For the distillate of the pre-concentration column D_0 from Fig. 5, we observe that (1) D_0 exhibits a non-linear effect on process TAC and varies in a very narrow range between 155.08 kmol/h and 155.38 kmol/h with a minimum TAC at 155.10 kmol/h, despite that we set D_0 belong to [140.00, 160.00] kmol/h. It demonstrates the existence of suitable distillate value range following process mass balance and product recovery. The suitable distillate values are narrow. (2) This is 1.31 kmol/h higher than the literature value $D_0 = 153.793$ kmol/h (case 2). It happens because the case 2 design suffers the specification of 0.65 mol fraction acetonitrile in D_0 stream. Our choice of releasing that constraint improves the product recovery slightly. In more details, Table 3 shows that the acetonitrile composition in D_0 stream in case 3 (0.6447) is very close to that in case 2 (0.65). That marginal difference is fortuitous and not forced by any constraints. Conjugated to a reduction of the pressure it increases significantly the relative volatility of acetonitrile over water in D_0 stream in case 3 whereas that in case 2 it is near unity since at $P_0 = 1$ atm, 0.65 is approximately the azeotrope composi-

tion (Table 3). Consequently, the number of trays and the reflux ratio needed to obtain a distillate with such low relative volatility are lower for case 3 comparing with that for case 2 (see Table 2 and 4).

For the distillate of the regeneration column, we see that the D_2 design range is as narrow as D_0 's one, again with a minimum for TAC at 55.14 kmol/h, despite the fact that D_2 could vary from 49.00 to 58.00 kmol/h. D_2 in the case 3 design is higher than that in case 2. This is a consequence of the fact that more water enters in D_0 stream, percolates in the extractive column bottom to enter the regeneration column where it is separated from the entrainer.

3.2.5. Comparison of final design parameters

Since there are four objective functions, we select the designs in Pareto front named case 3, 4, 5 and 6 with the lowest TAC, the lowest GEC, the highest E_{ext} and the highest e_{ext} , respectively. The parameters of the selected designs are shown in Table 4, referring to the notations in Fig. 1. The related sizing parameters and the cost data are shown in Table B in Appendix B.

Comparing the literature design (Table 2) with our design case 3 in Table 4, we find a significant improvement through decreasing the operating pressures of three columns. Comparing case 3 with case 2, the entrainer flow rate is reduced by 39.3%, from 145 kmol/h to 88 kmol/h which enables together with the reflux ratio reductions in the preconcentration and regeneration column, and the pressure reduction lowering the boiling temperatures to decrease the global energy consumption to drop by 25.6%.

From the process economic view, TAC is reduced by 20.8% thanks to the decrease of entrainer flow rate, column diameters, column tray number (32 trays less in total), heat exchanger areas and total reboiler duty. Going into more details, for the pre-concentration column, a 34.4% reduction of the column shell cost I_{CS} from Table B in Appendix B is mainly contributed by the decrease of the column tray number N_p although the column diameter is increased. Meanwhile, the operating cost is reduced by 22.1% because of the decrease of R_0 . The small value of R_0 indicates that the pre-concentration column works like a stripper with nearly no reflux flow rate. The result indicates that imposing the constraint of distillate purity (like being at the azeotropic composition) on the pre-concentration column is unsuitable. On the other hand,

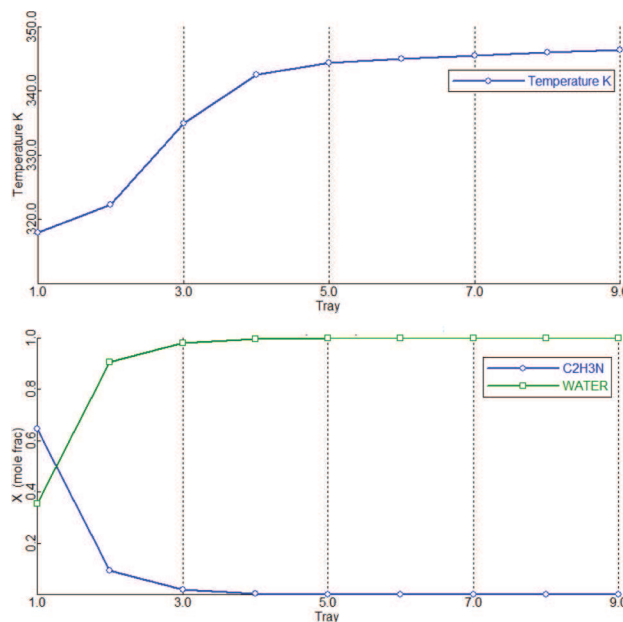


Fig. 6. Temperature and composition profiles of pre-concentration column for the extractive distillation of acetonitrile (C2H3N) – water with ethylene glycol (EG), case 3.

the condenser heat exchanger area is increased threefold due to the decrease of the condenser temperature at a lower pressure. Overall, the saving of the column annual cost $Cost_{CA}$ for pre-concentration column in case 3 reaches 16.6%. For the extractive column, the shell cost I_{CS} and heat exchanger cost I_{HE} in case 3 are reduced by 8.2% and 38.5% compared with that in case 2, respectively. It is because of the decreases of the column height and of the condenser heat transfer area A_R , caused by the increase of temperature driving force and the decrease of the operating pressure. A lower pressure reduces the reboiler duty and induces a decrease by 26.6% of the operating cost $Cost_{ope}$. For regeneration column, the annual cost is cut down by 17.3% thanks to a 52% reduction of operating cost due to less entrainer entering the column, although the capital cost is increased by 18.0% caused by the increase of the reboiler heat exchanger area.

Following the definition of E_{ext} and e_{ext} (You et al., 2015b), case 3 provides values for the suitable efficiency indicators E_{ext} as 0.211 and e_{ext} as 0.0081. With respect to energy consumption, case 3 is 1.1% higher than the minimum GEC case 4. That latter shows a 2.5% higher TAC because more trays are employed in the extractive column. Case 4 uses less energy due to slightly lower reflux ratios in the extractive and regeneration columns. Obviously, there is a

trade-off between capital cost and operating cost. These results prove that minimizing TAC and GEC is not equivalent. This motivated our choice of setting two distinct objectives in our optimization problem.

Regarding now case 5 and 6. They correspond to the maximum total E_{ext} and per tray e_{ext} extractive separation efficiency. In agreement with You et al. (2015), maximizing those indicators alone is not recommended for finding a proper design. Indeed, in accordance to their definition (see Section 2.2.3) doing that kind of optimization forces the extractive section profile to cover the whole feasible region of the extractive section. In agreement with the thermodynamic insights discussed in the literature (Rodriguez-Donis et al., 2011; Gerbaud and Rodriguez-Donis, 2014; Petlyuk et al., 2015) that requires mostly an increase in reflux ratio since that is the main driver of the feasible region area. Then the tray number and entrainer flow rate adjust themselves to maximize the extent of the extractive section composition profile. Rather than reaching an extremum, a suitable value exist (see case 3), as was noticed by De Figueiredo et al., 2015a, 2015b who suggested to set the within an suitable range the solvent composition in the solvent feed tray, one of the bounds used to computed the extractive separation efficiencies (see also discussion in Section, 3.2.6).

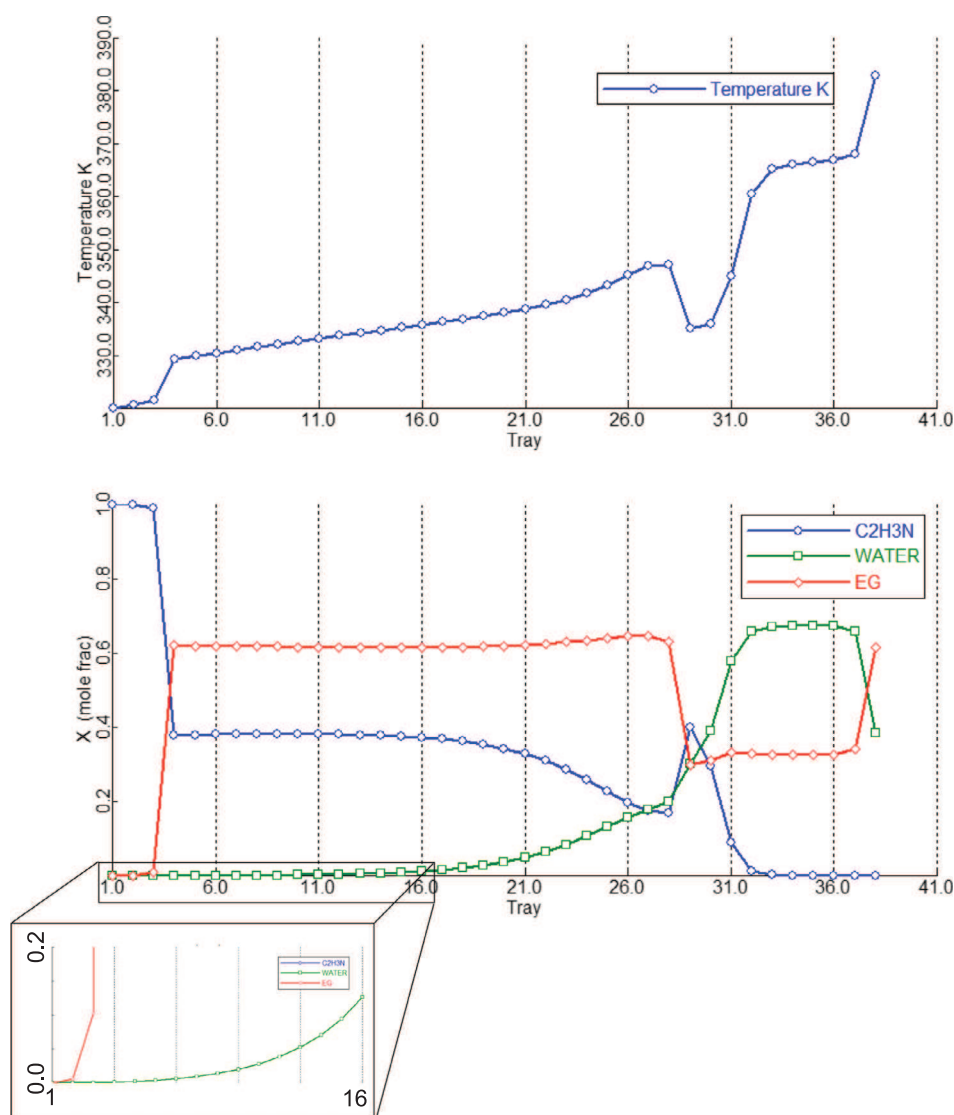


Fig. 7. Temperature and composition profiles of extractive column for the extractive distillation of acetonitrile (C2H3N) – water with ethylene glycol (EG), case 3.

Another interesting point is that more distillate of acetonitrile with the same purity specification is obtained in our design compared with case 2 even though the entrainer flow rate, tray number of columns and energy consumption are all reduced dramatically. We attribute that benefit to the operation of the columns at lower pressure. That enhances the relative volatility in all columns and the separation is easier, esp. in the regeneration column where the entrainer recycle has less impurity. Your relation between the product recovery and recycle stream impurity show that less impurity boosts up the extractive column distillate output (You et al., 2016b).

The temperature and composition profiles of the pre-concentration, extractive and regeneration columns of case 3 design are shown in Figs. 6–8.

In the pre-concentration column, the stripping and the rectifying section contains seven and two trays respectively. The small rectifying section is enough because the distillate composition is far from the azeotrope at low pressure as seen from Table 3. It is worth stressing that unlike the usual belief (e.g. literature's reference case from Liang et al., 2014) the design case 3 does not require feeding the extractive column with an azeotropic feed coming from D_0 . For the extractive column, the entrainer feed temperature (specified at 320 K) is suitable, but the fresh feed (D_0) temperature is much lower than that of the related feed tray, resulting in the large heat duty difference between the reboiler and condenser. It hints that preheating the fresh feed should be considered for reducing the reboiler duty Q_{R1} , but we did not consider it in this study.

The short rectifying section implies that the relative volatility of acetonitrile over EG is high enough. In the extractive section, the water content seems flat from tray number 16 to 4. But zooming in Fig. 7 shows that each tray is needed to prevent water entering the rectifying section, because of the high acetonitrile product purity specification at 0.9999. Like other extractive separations of 1.0-1a mixtures, this proves the statement that the stable node of extractive section SN_{ext} should be as close as to the entrainer-product edge for achieving high purity product as obtained from thermodynamic insight (Rodriguez-Donis et al., 2009). Down the column, the stripping section prevents acetonitrile entering W_2 from Fig. 7 and the remixing of water and EG is observed. Lastly, the regeneration column works well for recycling entrainer EG as seen from its temperature and composition profile diagrams.

3.2.6. Insight from ternary maps and relative volatility diagrams

Fig. 9 shows the ternary liquid composition profiles for case 2, 3, 5 and 6 in the extractive column of acetonitrile – water with EG. The ternary map of case 4 is similar to that of case 3. Those maps are useful to locate the suitable profiles and compare it to the feasible region of extractive section profiles analyzed by several authors (Rodriguez-Donis et al., 2009; Gerbaud and Rodriguez-Donis, 2014; Petlyuk et al., 2015).

Fig. 10 displays the relative volatility of acetonitrile vs water through the extractive column for case 2, 3, 4, 5 and 6. Case 1 is not shown in Figs. 9 and 10 since it does not reach the product

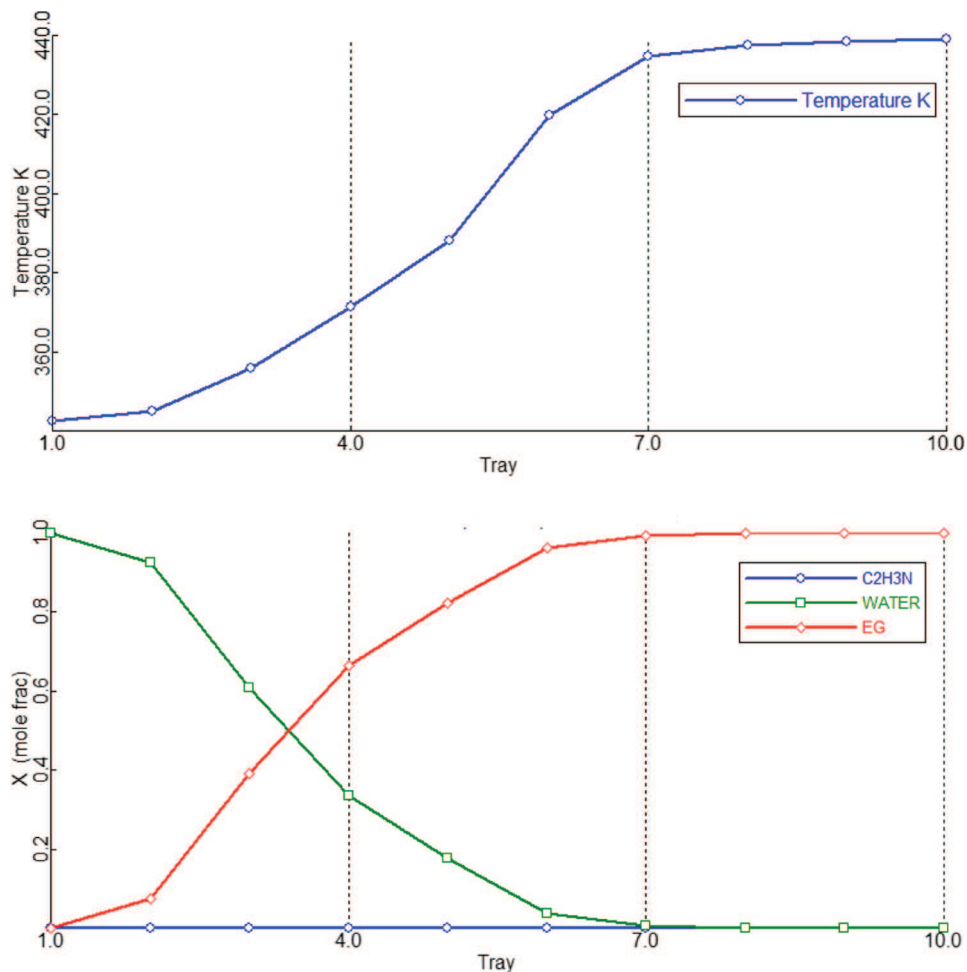


Fig. 8. Temperature and composition profiles of regeneration column for the extractive distillation of acetonitrile (C2H3N) – water with ethylene glycol (EG), case 3.

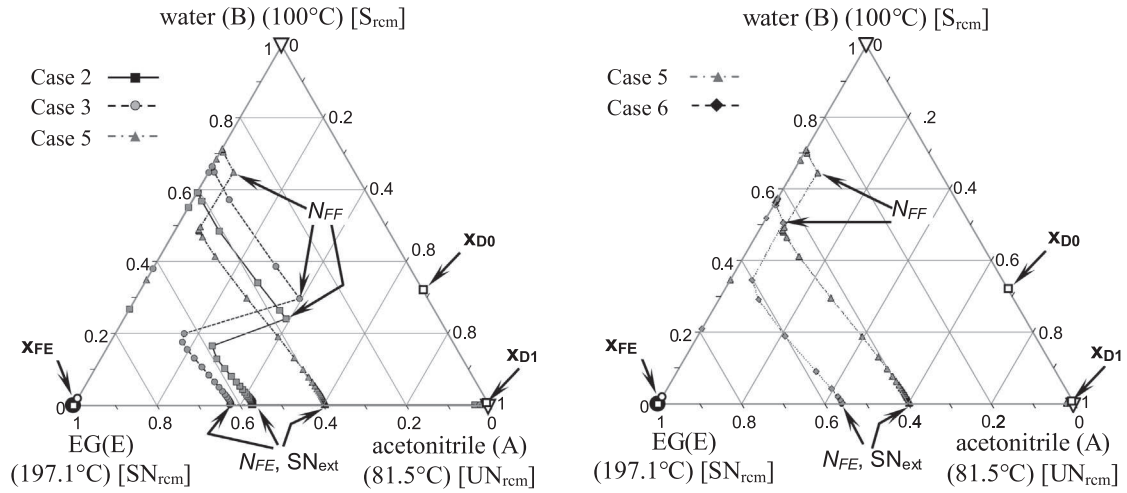


Fig. 9. Ternary liquid composition profiles for case 2, 3, 5 and 6 in the extractive column of acetonitrile – water with EG.

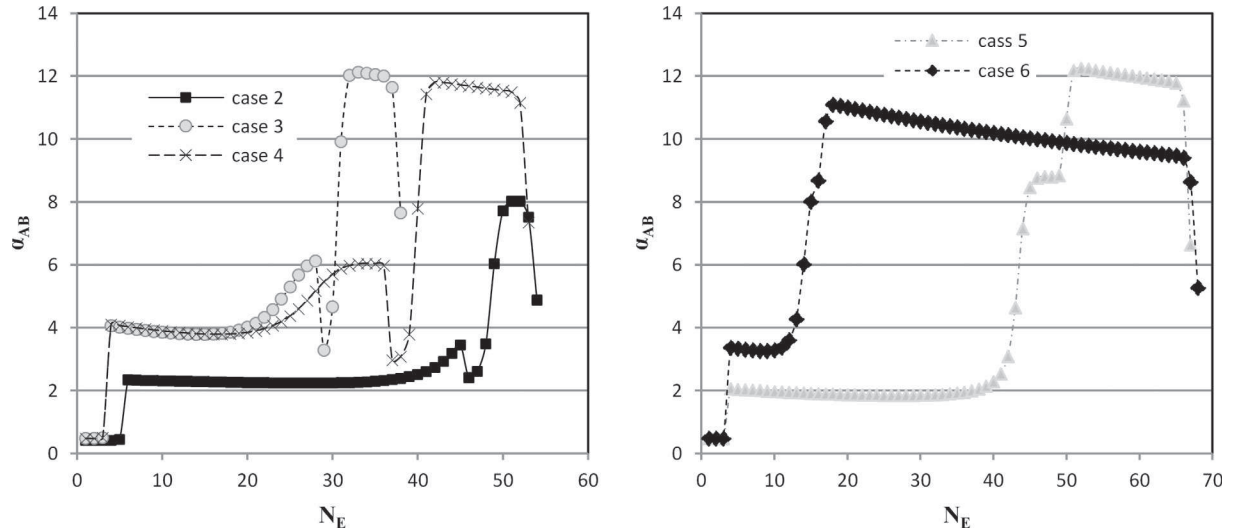


Fig. 10. Relative volatility of acetonitrile (A) vs water (B) through the extractive column for case 2, 3, 4, 5 and 6, acetonitrile – water with EG.

purity specification when taking the pressure drop per tray into account.

From Fig. 9, we observe that (1) the stable node of extractive section SN_{ext} at entrainer feed tray N_{FE} are very close to the BE side, and it demonstrates that this must occur to get a high purity product. (2) Less trays used in the rectifying section suggest that the separation between acetonitrile and EG is easy. (3) Analysis of the location of SN_{ext} (N_{FE} arrow in Fig. 9) for case 3 is interesting as this is one of the constraint De Figueiredo et al., 2015a, 2015b suggested to constraint it between 0.2 and 0.75 for a good extractive distillation design. First, it lies for all cases within that range. Hence, we conclude that De Figueiredo's range is too large to be used as a guidance. Second, it should be closer for case 3 at first glance to the acetonitrile vertex due to a lower F_E compared with case 2. That happens for case 5 and 6 in Fig. 9. However, the opposite happens for case 2 and 3 because the location of SN_{ext} is also determined by the reflux ratio R_1 , and it could be pushed toward product acetonitrile point by decreasing F_E or increasing R_1 , as evidenced in the literature (Knapp and Doherty, 1994; Petlyuk et al., 2015). Therefore, there are competitiveness and trade-off between F_E and R_1 for determining the location of SN_{ext} .

The extremum points N_{FF} and N_{FE} of the extractive profiles in Fig. 9 are used to compute the efficiency indicators (Eqs. (3 and 4)) reported in Tables 2 and 4. The largest E_{ext} value (case 5) and a high one (case 6) show that the feasible region of extractive distillation gets larger as we increase F_E and R_1 (like case 5 and 6). Although feasibility is enhanced, high F_E and R_1 raises the process TAC and the energy consumption. The best design is a trade-off between a feasibility governed by thermodynamics through composition profiles and process cost and energy demands.

The relative volatility maps in the extractive column displayed in Fig. 10 help understand the process operation. First for all design cases, $\alpha_{acetonitrile \text{ vs water}} = \alpha_{AB} > 1.8$ in the extractive section, showing that the addition of entrainer has enhanced the volatility towards and enabled the recovery of A, acetonitrile as distillate. In the rectifying section $\alpha_{AB} < 1$ and the water impurity of acetonitrile product may accumulate and pollute the acetonitrile product in D_1 . This is the reason why a high purity recycled entrainer with as low water as possible is needed and why so many trays in C1's extractive section are needed to prevent water to enter the rectifying section. In the extractive section, α_{AB} for case 2 with higher F_E and R_1 is lower than that in case 3. This happens because case 3 is operated at 0.3 atm rather than 1 atm and reducing the pressure

increases α_{AB} . With similar pressure, F_E and R_I , case 3 and 4 display similar α_{AB} values. Case 5 and 6, with very high extractive separation efficiencies are similar to each other and achieve relative volatilities up to 12. Again this shows that for extractive distillation, high F_E and R_I are harmful rather than useful for the separation once their optimal values are surpassed. This observation agrees with the results shown in literature (Knapp and Doherty, 1994; You et al., 2015a; Petlyuk et al., 2015) for acetone-methanol with water system, and validated the statement that once F_E is higher than its minimum value, changing other variables like reflux ratio and feed locations is a better way to approach a suitable design (Gerbaud and Rodriguez-Donis, 2014).

5. Conclusion

With the help of a multi-objective genetic algorithm, we have completed the design of an extractive distillation process for separating the acetonitrile – water azeotropic mixture with EG as entrainer (1.0-1a extractive separation class). For the first time we have investigated specifically five aspects simultaneously that have been optimized. (1) the pre-concentration column has been included and (2) no distillate composition constraint (like being at the azeotropic composition) in the pre-concentration column has been set. (3) The operating pressure has been allowed to be lower than 1 atm as this might usually enhance volatility for 1.0-1a class system. (4) A closed loop optimization was run, to handle the effect of impurity in the entrainer recycle, because earlier of our works have shown that too much impurity limits the main product recovery and purity from the extractive column. (5) the three columns process was optimized together and with multiple objectives, including separately two process criteria, the total annual cost and the global energy consumption, and two thermodynamics related separation efficiency indicators. Overall, 17 variables are optimized; column trays, all feed locations, refluxes, entrainer flow rate and all distillate products; under purity constraints for the acetonitrile and water product and for the entrainer recycle impurity.

Through the optimization, the Pareto front was obtained with nearly 400 designs satisfying the purity specifications. 169 designs exhibited a lower TAC than that a literature design value chosen as reference case 1 and modified to include pressure drop as case 2. For the design case 3, both the energy consumption and the TAC were reduced by more than 20% thanks to smaller entrainer flow rate, along with a reduction of 32 trays. All five aspects considered at the same time have been discussed and their value has been evidenced when attempting to perform an extractive distillation process optimization. We have shown that TAC and global energy consumption objectives give close but distinct design parameters and it is recommended to consider them distinctly at the same time.

Analyzing the extractive separation efficiency indicators, we have shown that they depended upon the F_E and R_I variables. Further analysis of maps of relative volatility in the extractive column illustrated that too high F_E and R_I are harmful rather than useful for

the separation once their minimum values are surpassed. Indeed, the best design is a trade-off between a feasibility governed by thermodynamics through composition profiles and process cost and energy demands.

Acknowledgment

This work was supported by the National Basic Research Program of China (2015CB251401), the Doctoral Fund of Ministry of Education of China (No. 2016M601528), the National Natural Science Foundation of China (No. 21706062).

Appendix A

The diameter of a distillation column is calculated using the *tray sizing* tool in Aspen Plus software.

The height of a distillation column is calculated from the equation:

$H = \frac{N}{e_T} \times 0.6096$ N tray stage except condenser and reboiler, e_T tray efficiency is taken as 85% for calculating TAC.

The heat transfer areas of the condenser and reboiler are calculated using following equations:

$A = \frac{Q}{u \times \Delta T}$ u: overall heat transfer coefficient ($\text{kW K}^{-1} \text{m}^{-2}$), $u = 0.852$ for condenser, 0.568 for reboiler.

The capital costs of a distillation column are estimated by the following equations:

Shell cost $t = \left(\frac{CEPCI}{100}\right) \times 902.8 \times D^{1.066} H^{0.802} \times (2.18 + F_C) = 22688.6 D^{1.066} H^{0.802}$ Unit of D and H: m

Tray cost $t = \left(\frac{CEPCI}{100}\right) \times 93.1 \times D^{1.55} H F_C = 1426.0 D^{1.55} H$ Unit of D and H: m

Heat Exchanger cost $t = \left(\frac{CEPCI}{100}\right) \times 457.4 \times A^{0.65} \times (2.29 + F_C) = 9367.8 A^{0.65}$ Unit of A: m^2

Appendix B

See Tables A–C.

Table A

The built-in binary parameters of NRTL model for acetonitrile – water with EG.

Component			
i	Acetonitrile	Acetonitrile	Water
j	Water	EG	EG
aij	−0.1164	0	0.3479
aji	1.0567	0	−0.0567
bij	256.4588	536.542	34.8234
bji	283.4087	130.1648	−147.137
cij	0.3	0.3	0.3

Table B

Sizing parameters and cost data of three columns extractive distillation for acetonitrile – water with EG.

Column	Case 1			Case 2			Case 3		
	C_0	C_1	C_2	C_0	C_1	C_2	C_0	C_1	C_2
Diameter/m	1.010	0.956	0.827	1.034	1.037	0.840	1.123	1.259	1.020
Height/m	10.37	37.80	12.20	10.37	37.80	12.20	5.49	26.22	6.10
$I_{CS}/10^6 \$$	0.150	0.399	0.138	0.154	0.435	0.140	0.101	0.399	0.099
A_C/m^2	40	29	13	42	34	14	126	96	23
A_R/m^2	62	302	36	67	337	38	34	56	94

Table B (continued)

Column	Case 1			Case 2			Case 3		
	C ₀	C ₁	C ₂	C ₀	C ₁	C ₂	C ₀	C ₁	C ₂
$I_{HE}/10^6$ \$	0.240	0.470	0.146	0.251	0.508	0.151	0.312	0.312	0.251
$Cost_{cap}/10^6$ \$	0.405	0.918	0.297	0.420	0.999	0.304	0.422	0.764	0.359
$Cost_{ope}/10^6$ \$	0.422	0.400	0.287	0.443	0.447	0.296	0.345	0.328	0.209
$Cost_{CA}/10^6$ \$	0.557	0.705	0.386	0.583	0.78	0.397	0.486	0.583	0.328
Q_{HA}/MW	1.067	1.074	0.487						
$Cost_{HA}/10^6$ \$	0.021	0.021	0.013						
$TAC/10^6$ \$	1.669	1.781	1.410						
Column	Case 4			Case 5			Case 6		
	C ₀	C ₁	C ₂	C ₀	C ₁	C ₂	C ₀	C ₁	C ₂
Diameter/m	1.123	1.249	1.020	1.123	1.643	0.983	1.145	1.640	0.977
Height/m	5.49	36.58	6.10	11.59	46.94	11.59	17.07	47.55	17.07
$I_{CS}/10^6$ \$	0.101	0.516	0.099	0.183	0.844	0.159	0.256	0.851	0.216
A_C/m^2	126	94	23	126	161	26	132	160	28
A_R/m^2	34	61	90	37	119	133	40	224	198
$I_{HE}/10^6$ \$	0.312	0.318	0.246	0.316	0.466	0.304	0.328	0.574	0.374
$Cost_{cap}/10^6$ \$	0.422	0.907	0.354	0.519	1.455	0.479	0.613	1.570	0.613
$Cost_{ope}/10^6$ \$	0.345	0.327	0.200	0.351	0.536	0.231	0.369	0.633	0.267
$Cost_{CA}/10^6$ \$	0.486	0.629	0.318	0.524	1.020	0.390	0.574	1.157	0.471
Q_{HA}/MW	0.472	0.58	1.199						
$Cost_{HA}/10^6$ \$	0.012	0.014	0.024						
$TAC/10^6$ \$	1.445	1.948	2.226						

Table CMinimum GEC and TAC, maximum E_{ext} and e_{ext} at different generations.

Number of generation	Statement	GEC (kJ/kmol)	TAC (10^6 \$)	E_{ext}	e_{ext}
0	Generating randomly the population (400)				
5	No design satisfies the constraints				
25	7 designs in Pareto front	220,972	1.890	0.336	0.0066
50	45 designs in Pareto front	178,683	1.741	0.432	0.0165
100	152 designs in Pareto front	163,185	1.568	0.511	0.0269
200	355 designs in Pareto front	159,458	1.472	0.552	0.0277
270	400 designs in Pareto front	157,897	1.440	0.553	0.0281
400	400 designs in Pareto front	156,749	1.413	0.553	0.0281
450	400 designs in Pareto front	156,628	1.410	0.553	0.0281
480	400 designs in Pareto front	156,628	1.410	0.553	0.0281

References

- Acosta-Esquivarosa, J., Rodríguez-Donis, I., Jáuregui-Haza, U., Nuevas-Paz, L., Pardillo-Fontdevila, E., 2006. Recovery of acetonitrile from aqueous waste by a combined process: solvent extraction and batch distillation. *Sep. Purif. Technol.* 52, 95–101.
- Arifin, S., Chien, I.L., 2008. Design and control of an isopropyl alcohol dehydration process via extractive distillation using dimethyl sulfoxide as an entrainer. *Ind. Eng. Chem. Res.* 47, 790–803.
- Armarego, W.L.F., Chai, C.L.L., 2013. Purification of Laboratory Chemicals. Butterworth-Heinemann.
- Bravo-Bravo, C., Segovia-Hernández, J.G., Gutiérrez-Antonio, C., Durán, A.L., Bonilla-Petriciolet, A., Briones-Ramírez, A., 2010. Extractive dividing wall column: design and optimization. *Ind. Eng. Chem. Res.* 49, 3672–3688.
- CEPCI., 2016. CEPCI index for year 2013. *Chemical engineering*, 123, 92.
- De Figueiredo, M.F., Guedes, B.P., de Araújo, J.M.M., Vasconcelos, L.G.S., Brito, R.P., 2011. Optimal design of extractive distillation columns—a systematic procedure using a process simulator. *Chem. Eng. Res. Des.* 89, 341–346.
- De Figueiredo, M.F., Brito, K.D., Ramos, W.B., Vasconcelos, L.G.S., Brito, R.P., 2015a. Effect of solvent content on the separation and the energy consumption of extractive distillation columns. *Chem. Eng. Commun.* 202, 1191–1199.
- De Figueiredo, M.F., Brito, K.D., Ramos, W.B., Vasconcelos, L.G.S., Brito, R.P., 2015b. Optimization of the design and operation of extractive distillation processes. *Sep. Sci. Tech.* 50, 2238–2247.
- Doherty, M.F., Knapp, J.P., 1993. Distillation, azeotropic, and extractive. *Kirk-Othmer Encycl. Chem. Technol.*
- Douglas, J.M., 1988. *Conceptual Design of Chemical Processes*. McGraw-Hill, New York.
- García-Herreros, P., Gómez, J.M., Gil, I.D., Rodríguez, G., 2011. Optimization of the design and operation of an extractive distillation system for the production of fuel grade ethanol using glycerol as entrainer. *Ind. Eng. Chem. Res.* 50, 3977–3985.
- Gerbaud, V., Rodríguez-Donis, I., 2014. Chapter 6. Extractive distillation. In: Gorak, A., Olujic, Z. (Eds.), *Distillation: Equipment and Processes*. Elsevier, Oxford, GB, pp. 201–246.
- Gomez, A., Pibouleau, L., Azzaro-Pantel, C., Domenech, S., Latge, C., Haubensack, D., 2010. Multiobjective genetic algorithm strategies for electricity production from generation IV nuclear technology. *Energy Convers. Manage.* 51, 859–871.
- Huang, K., Shan, L., Zhu, Q., Qian, J., 2008. Adding rectifying/stripping section type heat integration to a pressure-swing distillation (PSD) process. *Appl. Therm. Eng.* 28, 923–932.
- Knapp, J.P., Doherty, M.F., 1994. Minimum entrainer flows for extractive distillation: A bifurcation theoretic approach. *AIChE J.* 40, 243–268.
- Kossack, S., Kraemer, K., Gani, R., Marquardt, W., 2008. A systematic synthesis framework for extractive distillation processes. *Chem. Eng. Res. Des.* 86, 781–792.
- Leboreiro, J., Acevedo, J., 2004. Processes synthesis and design of distillation sequences using modular simulators: a genetic algorithm framework. *Comput. Chem. Eng.* 28, 1223–1236.
- Li, L., Guo, L., Tu, Y., Yu, N., Sun, L., Tian, Y., Li, S., 2017. Comparison of different extractive distillation processes for 2-methoxyethanol/toluene separation: Design and control. *Comput. Chem. Eng.* 99, 117–134.
- Liang, K., Li, W., Luo, H., Xia, M., Xu, C., 2014. Energy-efficient extractive distillation process by combining preconcentration column and entrainer recovery column. *Ind. Eng. Chem. Res.* 53, 7121–7131.
- Luyben, W.L., 2012. Pressure-swing distillation for minimum-and maximum-boiling homogeneous azeotropes. *Ind. Eng. Chem. Res.* 51, 10881–10886.
- Luyben, W.L., Chien, I.L., 2011. *Design and Control of Distillation Systems for Separating Azeotropes*. John Wiley & Sons.
- Luyben, W.L., 2016. Distillation column pressure selection. *Sep. Pur. Tech.* 168, 62–67.
- Mahdi, T., Ahmad, A., Nasef, M.M., Ripin, A., 2015. State-of-the-art technologies for separation of azeotropic mixtures. *Sep. Purif. Rev.* 44, 308–330.
- Ortiz, P.S., Oliveira, S., 2014. Exergy analysis of pretreatment processes of bioethanol production based on sugarcane bagasse. *Energy* 76, 130–138.

- Petlyuk, F., Danilov, R., Burger, J., 2015. A novel method for the search and identification of feasible splits of extractive distillations in ternary mixtures. *Chem. Eng. Res. Des.* 99, 132–148.
- Rangaiah, G.P., 2009. *Multi-Objective Optimization: Techniques and Applications in Chemical Engineering*. World scientific.
- Rangaiah, G.P., Bonilla-Petriciolet, A., 2013. *Multi-Objective Optimization in Chemical Engineering: Developments and Applications*. John Wiley & Sons.
- Rangaiah, G.P., Sharma, S., Sreepathi, B.K., 2015. Multi-objective optimization for the design and operation of energy efficient chemical processes and power generation. *Curr. Opin. Chem. Eng.* 10, 49–62.
- Repke, J.U., Forner, F., Klein, A., 2005. Separation of homogeneous azeotropic mixtures by pressure swing distillation—analysis of the operation performance. *Chem. Eng. Technol.* 28, 1151–1157.
- Rodríguez-Donis, I., Gerbaud, V., Joulia, X., 2009. Thermodynamic insights on the feasibility of homogeneous batch extractive distillation, 1. Azeotropic mixtures with a heavy entrainer. *Ind. Eng. Chem. Res.* 48, 3544–3559.
- Rodríguez-Donis, I., Gerbaud, V., Joulia, X., 2011. Thermodynamic insights on the feasibility of homogeneous batch extractive distillation. 3. Azeotropic mixtures with light entrainer. *Ind. Chem. Eng. Res.* 51, 4643–4660.
- You, X., Rodríguez-Donis, I., Gerbaud, V., 2015a. Improved design and efficiency of the extractive distillation process for acetone–methanol with water. *Ind. Eng. Chem. Res.* 54, 491–501.
- You, X., Rodríguez-Donis, I., Gerbaud, V., 2015b. Investigation of separation efficiency indicator for the optimization of the acetone–methanol extractive distillation with water. *Ind. Eng. Chem. Res.* 54, 10863–10875.
- You, X., Rodríguez-Donis, I., Gerbaud, V., 2016a. Reducing process cost and CO₂ emissions for extractive distillation by double-effect heat integration and mechanical heat pump. *Appl. Energy* 166, 128–140.
- You, X., Rodríguez-Donis, I., Gerbaud, V., 2016b. Low pressure design for reducing energy cost of extractive distillation for separating diisopropyl ether and isopropyl alcohol. *Chem. Eng. Res. Des.* 109, 540–552.
- Zhu, Z., Wang, L., Ma, Y., Wang, W., Wang, Y., 2015. Separating an azeotropic mixture of toluene and ethanol via heat integration pressure swing distillation. *Comput. Chem. Eng.* 76, 137–149.